


Article

Point of Zero Charge: Role in Pyromorphite Formation and Bioaccessibility of Lead and Arsenic in Phosphate-Amended Soils

Ranju R. Karna ^{1,2}, Matthew R. Noerpel ^{1,2}, Todd P. Luxton ²  and Kirk G. Scheckel ^{2,*}

¹ Oak Ridge Institute for Science and Education, Oak Ridge, TN 37830, USA; karna.ranju@epa.gov (R.R.K.); Noerpel.Matt@epa.gov (M.R.N.)

² United States Environmental Protection Agency, National Risk Management Research Laboratory, Cincinnati, OH 45224, USA; luxton.todd@epa.gov

* Correspondence: Scheckel.Kirk@epa.gov; Tel.: +1-513-487-2865

Received: 1 March 2018; Accepted: 6 April 2018; Published: 14 April 2018



Abstract: Soluble lead (Pb) can be immobilized in pure systems as pyromorphite through the addition of phosphorus (P) sources; however, uncertainties remain in natural systems. Knowledge of point zero charge (PZC) is important to predict the ionization of functional groups and their interaction with metal species in solution. This study utilized Pb- and As-contaminated soils to determine the combined effect of pH with respect to PZC and different rates of P-application on pyromorphite formation as well as Pb and arsenic (As) bioaccessibility as impacted by speciation changes. Solution chemistry analysis along with synchrotron-based Pb- and As-speciation as well as bioaccessibility treatment effect ratios (TERs) were conducted. Results indicated no significant effect of PZC on pyromorphite formation in P-amended soils; however, the TER_{Pb} appeared significantly lower at $pH > pH_{PZC}$ and higher at $pH < pH_{PZC}$ ($\alpha = 0.05$). In contrast, the TER_{As} was significantly higher at $pH > pH_{PZC}$ compared to the other two treatments for the tested soils. The lack of conversion of soil Pb to pyromorphite may be attributed to several reasons including the presence of highly stable minerals, such as plumbojarosite, limiting soluble Pb availability to react with phosphates, high Fe and S content in IKS, high organic matter in BO, and high Ca content in NW.

Keywords: lead immobilization; pyromorphite; point zero charge; treatment effect ratio; lead speciation

1. Introduction

Lead is toxic to humans, especially to young children and animals [1]. Lead contamination of soil is so pervasive that excavation and subsequent back-filling with clean soil is unsustainable, very costly, and requires an impractically large volume of clean soil. Therefore, alternative approaches are required to protect the human lives that are in regular contact with Pb-impacted soils. Alteration of Pb species can significantly benefit humans and environmental health by reducing its toxicity even if the total Pb concentration may remain the same [2,3]. Amending Pb-contaminated soils with phosphorus (P) as an in situ remediation option has been proposed as an alternative to soil removal [4]. For the cases of Pb-contaminated sites, evidence has shown that phosphorous (P) compounds have been used to form highly insoluble, highly stable Pb precipitates that are not biologically available [5–12]. With sufficient availability of P, Pb salts and inorganic Pb-bearing minerals such as anglesite ($PbSO_4$), cerussite ($PbCO_3$), and galena (PbS) spontaneously transform into pyromorphite ($Pb_5(PO_4)_2Cl,OH$). Pyromorphite is several orders of magnitude less soluble than the most commonly found Pb minerals in soils, suggesting that the transformation of soil Pb to pyromorphite would reduce the bioavailability

and therefore toxicity of Pb. Soluble Pb can be immobilized in pure systems as pyromorphite by adding sources of P; however, doubts remain about the efficacy of this approach in natural soil systems [10,11]. The possibility of inadequate immobilization or the dissolution of pyromorphite after P-amendments have also been reported [12,13]. In general, pyromorphite formation is controlled by a soil solution P that is dominated by orthophosphate species which are influenced by solution pH ($\text{H}_3\text{PO}_4^0 \rightarrow \text{H}_2\text{PO}_4^{1-} \rightarrow \text{HPO}_4^{2-} \rightarrow \text{PO}_4^{3-}$ as pH increases). Solution pH is directly tied to the acid dissociation constants (pKa) of phosphoric acid (H_3PO_4^0), indicating that at solution pH less than 2.12, H_3PO_4^0 is the dominant species. Between pH 2.12 and 7.21, H_2PO_4^- is prominent and above pH 7.21 to 12.38, HPO_4^{2-} is present [9]. Thermodynamically, pyromorphite formation is favored when H_3PO_4^0 and H_2PO_4^- are present. Therefore, it is believed that a lower soil pH may need to be maintained to enhance soil Pb transformation to pyromorphite. Despite studies which utilized a lower soil pH during P-amendments, formation of pyromorphite has not been favored as expected. Likewise, the application of phosphate fertilizers in Pb and As co-contaminated soil has been correlated with increased As mobility [14,15] due to sorption site competition between arsenate (AsO_4^{3-}) and phosphate (PO_4^{3-}). Care should be taken when considering phosphate amendments to sequester Pb as other elements may become more mobile and result in adverse effects.

Consideration of native soil pH, organic matter content, and water holding capacity have been explored, but little has been examined on external controls to alter the soil environment prior to phosphate amendments. The pH at which the sorbent surface charge assumes a zero value is defined as the point of zero charge (pH_{PZC}). At this pH, the sum charge of the positive surface sites is equal to that of the negative ones resulting in a high state of entropy and disequilibrium. The knowledge of pH_{PZC} helps to hypothesize on the ionization of functional groups and their interaction with metal species in solution. At solution pHs higher than pH_{PZC} , sorbent surface is negatively charged and can interact with positively charged metal species. However, at pHs lower than pH_{PZC} , solid surface is positively charged and can interact with negative species [16]. We theorized that driving the pH of a soil system to a state of disequilibrium may enhance contaminant immobilization.

Potentiometric titration method is more commonly used in soils having surfaces dominated by variable charge colloids. Point zero salt effect, defined as a distinct point (pH) at the intersection of titration curves generated for different concentrations of non-specifically adsorbing electrolytes, was measured for all the tested soils in this study. A detailed review and discussion of surface charging as well as the various points of zero charge are described in previous literature [17–19].

An essential aspect of in situ immobilization of Pb via phosphate amendments is to lower the risk (bioavailability) of Pb in soil. Bioavailability can be assessed with animal (in vivo) and simple chemical extraction assays (in vitro). As stated in EPA Method 1340, the assay at pH 1.5 is not suitable for phosphate-amended soils which overestimates Pb bioaccessibility in amended soils. The difference in Pb extractability at pH 1.5 versus pH 2.5 for phosphate-amended soils may be a result of a change in phosphate chemistry. Below pH 2.12, phosphate prefers to be H_3PO_4 ; above pH 2.12, phosphate prefers $\text{H}_2\text{PO}_4^{-1}$. A slight shift in extraction pH can have a profound effect on phosphate chemistry and extractability. Therefore, in vitro bioaccessibility assay (IVBA) extraction at both pH 1.5 and pH 2.5 following the standard IVBA procedure was conducted in the present study.

Any amendment is expected to alter the chemistry of metals present in soils and these changes should be measured and evaluated. Metal speciation identifies the changes in mineralogy and strongly determines the bioavailability on the basis of differences in the solubility of soil minerals [20,21]. Additional details on the advantages and successes of using synchrotron-based techniques in contaminated soils can be found in past studies [3,22–25], especially for speciation and quantification of Pb in P-amended soils.

The objective of this study was a comparison of the combined effects of pH with respect to PZC, an analysis of different rates of phosphate application on the formation and stability of pyromorphite over time, as well as how speciation changes have impacted Pb and As bioaccessibility. Attempts

have been made to fine-tune and understand the limitations of Pb conversion to pyromorphite in phosphate-amended soils.

2. Materials and Methods

2.1. Soil Characterization

This study evaluated soils contaminated with Pb and As such as BO (Orchard, NC, USA), IKS (mining-impacted, Dewey-Humboldt, AZ, USA), and NW (smelter-impacted, Lincoln, NE, USA). BO and IKS soils have been evaluated in previous studies for Pb and As bioaccessibility [26] and NW soil provided an opportunity to investigate Pb immobilization at a Superfund site. BO was collected from Haywood country in North Carolina where an orchard was in use from 1908 to 1988; during this time, a lead-arsenate pesticide was heavily used and, accordingly, the site is highly contaminated with Pb and As. All the tested soils were classified at county level using the NRCS-USDA soil classification database available online. BO was classified as fine-loamy, mixed, superactive, mesic Humic Hapludults. IKS soil was mining-impacted soil collected from Yavapai county, Arizona with very high Fe (~15%) and S (~8%), and about 2% organic matter content.

IKS was classified as fine-loamy, mixed, mesic Ustollic Haplargids. NW was collected from urban Lincoln, Nebraska and exhibited total Pb (1730 mg kg⁻¹), As (9 mg kg⁻¹), Mn (517 mg kg⁻¹), and Fe (2.5%). NW was classified as fine-silty, mixed, mesic Cumulic Hapludolls. All the tested soils were oven-dried and properly homogenized using sample splitter (# 1613, Carpco Inc., Texarkana, AR, USA) [27].

2.2. Physicochemical Characterization

The homogenized soil in triplicate were subjected to measure soil pH in water after being sieved and oven-dried. Total extractable solid digestion (US EPA Method 3051a) [28] was conducted on each soil to measure the total contents of Pb, As, Mg, Ca, Fe, P, and most of the transition metals by using inductively coupled plasma–optical emission spectroscopy (ICP-OES, ICP-6500 Trace Analyzer, Thermo Scientific, Waltham, MA, USA). Certified standard reference material (NIST 2710A) was digested and analyzed along with the samples with an acceptance range of ±10% of the certified value to verify the precision and accuracy in sample preparation and analysis. Total Pb and As concentrations were determined for BO (2065, 308 mg kg⁻¹), NW (1730, 19 mg kg⁻¹), and IKS (2462, 3958 mg kg⁻¹) ($n = 4$), respectively (Table 1).

Table 1. Total element contents of IKS (IKJ 583), NW soils, and BO determined in <250 μm size by using microwave-assisted acid digestion (EPA 3051A).

Soil Label	IKS	NW	BO
Source	Mining Slag (mg kg ⁻¹)	Smelter Impacted (mg kg ⁻¹)	Pesticide Spray Lead Arsenate (mg kg ⁻¹)
Al	11,378	15,653	42,342
As	3958	19	308
Ca	26,648	14,453	5275
Cd	9	6	0.1
Co	10	10	19
Cr	<DL	26	106
Cu	327	513	212
Fe	138,400	25,010	38,874
Mg	9074	3431	11,405
Mn	408	517	1590
P	952	1354	1472
Pb	2462	1730	2065
Zn	4195	2141	180
S	85,864	1582	858

Overall, IKS was high in Fe and S, NW had slightly elevated Ca levels compared to other elemental contents, whereas BO had very high organic matter content (~7.2%).

The point zero charge (PZC) was determined by following Sparks [29]. The selection of those specific pHs below and above pH_{PZC} were done based on the understanding of relationships and physiochemical interactions of different P species in soils at varying pHs.

2.3. Batch Experiment Setup and Sample Collection

The batch experiment for BO was modified into a short-term preliminary study prior to conducting any long-term batch experiment. The results obtained from this study exhibited no pyromorphite formation, possibly a result of the presence of high Fe oxides and high organic matter. Instead, IKS and NW soils were used for long-term batch experiment to provide a more controlled environment to determine the role of PZC in pyromorphite formation.

Each treatment combination had three replicates for IKS and NW, with only one for BO (preliminary experiment). About 800 mL of 0.01 M CaCl_2 solution was added to 1000 mL HDPE bottle with HDPE plastic caps which contained pre-weighed 16 g of soil (20 g/L). The required amount of phosphoric acid (H_3PO_4) was used to treat the samples at different levels of P-amendment. The desired pH range was maintained at those particular pHs using Mettler Toledo DL-50 *Graphix* via acid-base titration for the first three days. Once the samples were pH-adjusted, the bottles were loaded onto a tumbler to keep them mixed continuously. The pHs of solution matrix were monitored every 24 h for the first two weeks, every three days for a month, and every week until pHs were stabilized.

The incubated bottles were periodically sub-sampled at 1-day, 1-week, 1-month, 3-month, and 6-month periods for about 50 mL of suspension. While pipetting, the suspension was continuously stirred for homogeneous sampling. The solid and liquid phases were separated by centrifuging at 4000 rpm for 10 min. Aqueous samples collected from the batch experiment were filtered through 0.45 μm filters and separated into aliquots for both total dissolved elements and anions measurements and stored as required until analyzed by ICP-OES and ion chromatography (ICS 5000, Thermo Scientific, Waltham, MA, USA). The bulk soil samples obtained after centrifugation were frozen until freeze-dried for X-ray absorption spectroscopy (XAS) and in vitro bioaccessibility analyses.

2.4. Assessment of Pb and As Bioaccessibility

US EPA Method 1340 at pH 1.5 was used for an in vitro bioaccessibility test. A similar procedure was used for bioaccessibility assays conducted at pH 2.5 as the only alteration. The treatment efficacy was expressed as the ratio of the Pb bioaccessibility in the treated soil divided by the Pb bioaccessibility in the untreated soil (treatment effect ratio (TER)). Studies have reported TER range from P-treated soils as a minimum of 0.08 [5] to maximum of 1.16 [30] with a median value of 0.78. A TER value of one indicates that the treatment had no effect on Pb bioaccessibility; a TER value of <1 indicates a decrease in Pb bioaccessibility due to treatment effect [31]. Median TER results indicated that P-amendments reduced Pb bioaccessibility but not significantly [5,30].

2.5. Quality Assurance and Quality Control (QA/QC) Checks

The accuracy of EPA Method 3051A digestion method was confirmed by a quantitative average of Pb recovery from NIST 2710A. During the determination of the Pb concentration in soil digests, triplicate analysis, spiked sample recoveries, and check values were included. In vitro bioaccessibility assessment included all the QA/QC checks as mentioned in the EPA method 1340. Details on QA/QC checks are provided in Table S1A,B.

2.6. XAS Data Collection and Analyses

X-ray absorption spectroscopy (XAS) was performed on all the treatment combinations in order to understand the Pb and As chemistry with different rates of P-amendment at different pH values at the Materials Research Collaborative Access Team (MRCAT) 10-ID for Pb [32] and 10-BM for

As [33] beamlines, Advanced Photon Source (Argonne National Laboratory, Lemont, IL, USA). For XAS data collection, the individual soil sample fractions (~100 mg) were mixed with 10 mg of polyvinylpyrrolidone (PVP) gently ground with an agate mortar and pestle to homogenize, pressed into a 1-cm pellet, and mounted onto Kapton tape. An integrated approach of solution chemistry analysis, XAS analysis, along with bioaccessibility assessments were conducted in order to meet the study objectives.

2.7. Statistical Analysis

To evaluate the broader trends across the three soils investigated, one- and two-way ANOVA tests were performed with a posthoc Tukey's means comparison. TER-As were normally distributed; however, the TER-Pb values were transformed by taking the square root of the value to achieve a normalized distribution of values. All analyses were performed in OriginPro 2015.

3. Results and Discussions

3.1. Effect of P-Amendment on Soil pH

When phosphoric acid (PA) was added to the soil suspensions, its influence on pH was variable depending on the buffering capacity of each individual soil. Soil pH (0.01 M CaCl₂) in IKS decreased from 3.66 to 2.84 (1% PA), 2.29 (5% PA), and 2.07 (10% PA). Soil pH (0.01 M CaCl₂) in NW decreased from 6.98 to 5.22 (1% PA), 3.25 (5% PA), and 2.29 (10% PA). Soil pH (0.01 M CaCl₂) in BO decreased from 5.60 to 4.05 (1% PA), 3.03 (5% PA), and 2.68 (10% PA). The highest buffering of pH was observed in BO due to the presence of high organic matter content. However, the desired pHs were maintained by adding potassium hydroxide (KOH) and hydrochloric acid (HCl) as required.

3.2. Pre-Amendment XAS-Based Pb- and As-Mineralogy in Tested Soils

The primary Pb mineral composition in pre-amended IKS included plumbojarosite (Pb_{0.5}Fe₃(SO₄)₂(OH)₆) and Pb sorbed to iron oxides. The other minor Pb minerals included Pb-phosphates and magnetoplumbite [Pb(Fe³⁺,Mn³⁺)₁₂O₁₉]. Lead bound to Fe (hydr)oxides was very common in a wide variety of environments in the presence of high Fe [34]. On the other hand, As in IKS was primarily associated with the weathering products of arsenic sulfide such as jarosite (52–70%), scorodite (hydrous ferrous arsenate) (31–38%), and As(V) ions sorbed on goethite (14–18%). Incorporation of As(V) in jarosite derived from the weathering of As-rich pyrite is well documented [35,36].

Lead-XAS data analysis on BO, which was contaminated with lead-arsenate (PbHAsO₄) pesticide, indicated Pb species mostly as sorbed phases to Fe (hydr)oxides and Pb complexed with humic acids as the minor component, which was expected in soil with high organic matter and high iron oxides. Arsenic speciation in BO included As(V) ions sorbed to birnessite (65–69%) and Pb–As pesticide (31–36%). More details on an initial mineralogy of IKS and BO can be referred to in R.R. Karna et al. [26]. Lead-XAS data analysis in NW indicated Pb bound to humic acids (75%) as the primarily dominant mineral; other minor minerals identified were anglesite (14%) and Pb sorbed to ferrihydrite (11%). Arsenic speciation in NW detected As(V) sorbed to goethite (28%), arsenopyrite (21%), As(V) sorbed to birnessite (20%), As(V) incorporated into jarosite (18%), and scorodite (13%).

3.3. Effect of P-Amendment and Different pHs on Pb- and As-Chemistry in Tested Soils

3.3.1. IKS (IKJ 583)

The ICP-OES analysis conducted on the effluent samples revealed no significant difference in total dissolved Pb in P-amended compared to non-amended treatments in IKS (Table S2), possibly a result of the lower solubility of Pb in soils. Interestingly, total dissolved As concentrations were lowest in the low P-amended treatments set at >pH_{PZC} indicating that the pH effect was more predominant

at low P-application in reducing the total dissolved As concentration in effluent samples. Decreasing soluble As concentration along with a decreasing soluble Ca concentration at $>pH_{PZC}$ (pH of 7) with medium and high P indicates higher possibilities of calcium arsenate formation which is more stable towards neutral pH, as reported by Bothe et al. [37]. Regarding the non-amended positive control (POS_CTRL), As solubility remained low and no pH effect was observed. However, high P-amendment demonstrated As mobilization, especially at pH_{PZC} (pH of 4) and $<pH_{PZC}$ (pH of 3). This observation may be self-evident because of the known effect of competitive adsorption mechanism between arsenate and phosphate that have similar deprotonation constants in solution and may have similar effects on the surface charge of the solid [38–42].

Considering initial Pb mineralogy, there were no significant changes in Pb species upon different rate of P-amendment in IKS at pH_{PZC} (pH of 4), $>pH_{PZC}$ (pH of 7), and $<pH_{PZC}$ (pH of 3). Plumbojarosite ($Pb_{0.5}Fe_3(SO_4)_2(OH)_6$) remained the primary geochemical phase across the treatment combinations. Other minor minerals included Pb sorbed to iron (hydr)oxides, lead phosphates ($Pb_3(PO_4)_2$), hydroxypyromorphite ($Pb_5(PO_4)_3OH$), and anglesite ($PbSO_4$). No particular trend in Pb-phosphate formations at $>pH_{PZC}$ was observed despite total soluble P displayed significant reduction at $>pH_{PZC}$. This indicates the possibility of insoluble calcium phosphate formation with the observed reduction in Ca-concentration at $>pH_{PZC}$ (Figure 1). Reduction in total soluble P at $>pH_{PZC}$ was also supported by the phosphate measurement in IKS (Table S5). Solubility of primary mineral phases of Pb and their reaction products with phosphate was very significant in determining the P-based remediation of Pb in contaminated soils [41]. For example, if the contaminated soils had more stable forms of Pb, dissolution rates for Pb were much slower. Studies have reported pyromorphite formation in the presence of different lead minerals and revealed that low pH (≤ 4) is favorable for cerussite dissolution and its conversion to pyromorphite [11]. High pH (>5) is favorable for dissolution of galena (PbS) and transformation of galena to pyromorphite [43]. Therefore, solubility of primary Pb solid phases and their reaction with phosphate cannot be neglected when assessing the efficiency of P-induced immobilization of soils [41]. However, for the IKS soil, Pb-mineralogy remained largely similar to the presence of plumbojarosite as a dominant mineral, despite the long (180-day) incubation.

Hindered dissolution of plumbojarosite in IKS may not have provided enough soluble Pb to react with phosphates for pyromorphite formation even after high P-amendment was applied at variable pHs. Despite the lack of pyromorphite formation, the bioaccessibility measurements for Pb indicated lower TERs estimations (0.16 to 0.52 via IVBA conducted at pH 2.5) in all the low, medium, and high P-amended treatments set at $>pH_{PZC}$ (Table 2).

Arsenic speciation in the original IKS was primarily associated with the weathering products of arsenic minerals, such as As_jarosite (52–70%), scorodite (hydrous ferrous arsenate) (31–38%), and As(V) ions sorbed on goethite (14–18%) [26]. Considering an initial As mineralogy, there were no significant changes in As-speciation upon different rates of P-amendment in IKS at pH_{PZC} (pH of 4), $>pH_{PZC}$ (pH of 7), and $<pH_{PZC}$ (pH of 3). However, As_jarosite was decreased to $<20\%$ and As(V) sorbed to goethite was increased to 32–47%, scorodite remained almost constant (Figure 2). The observed substantial repartitioning of As to the surface complexed fraction from its initially coprecipitated form (As_jarosite) indicates that As(V) in the current study was partially controlled by slow redox kinetics resulting in the Fe^{2+} -induced transformation of jarosite. Concurrently, it also led to the acceleration of the structural transformation of metastable Fe(III) minerals to subsequent precipitation of more stable phases, such as goethite, within 24 h in the presence of high Fe concentration. These results are also supported by previous studies [44–46]. The Fe^{2+} -induced transformation to Fe(III) oxides can enhance or impede mobilization and bioavailability of As [47]. Overall, there was a decrease in As_jarosite content by 32 to 44%, whereas increases in scorodite by approximately 10% and As_goethite formation by 28% were observed (Figure 2).

However, TERs estimations for As were lowest (0.41 at pH 1.5 and 0.68 at pH 2.5) for the treatments set at $<pH_{PZC}$, and, interestingly with high P-amendment despite similar As mineralogy across the treatment combinations (Table 2).

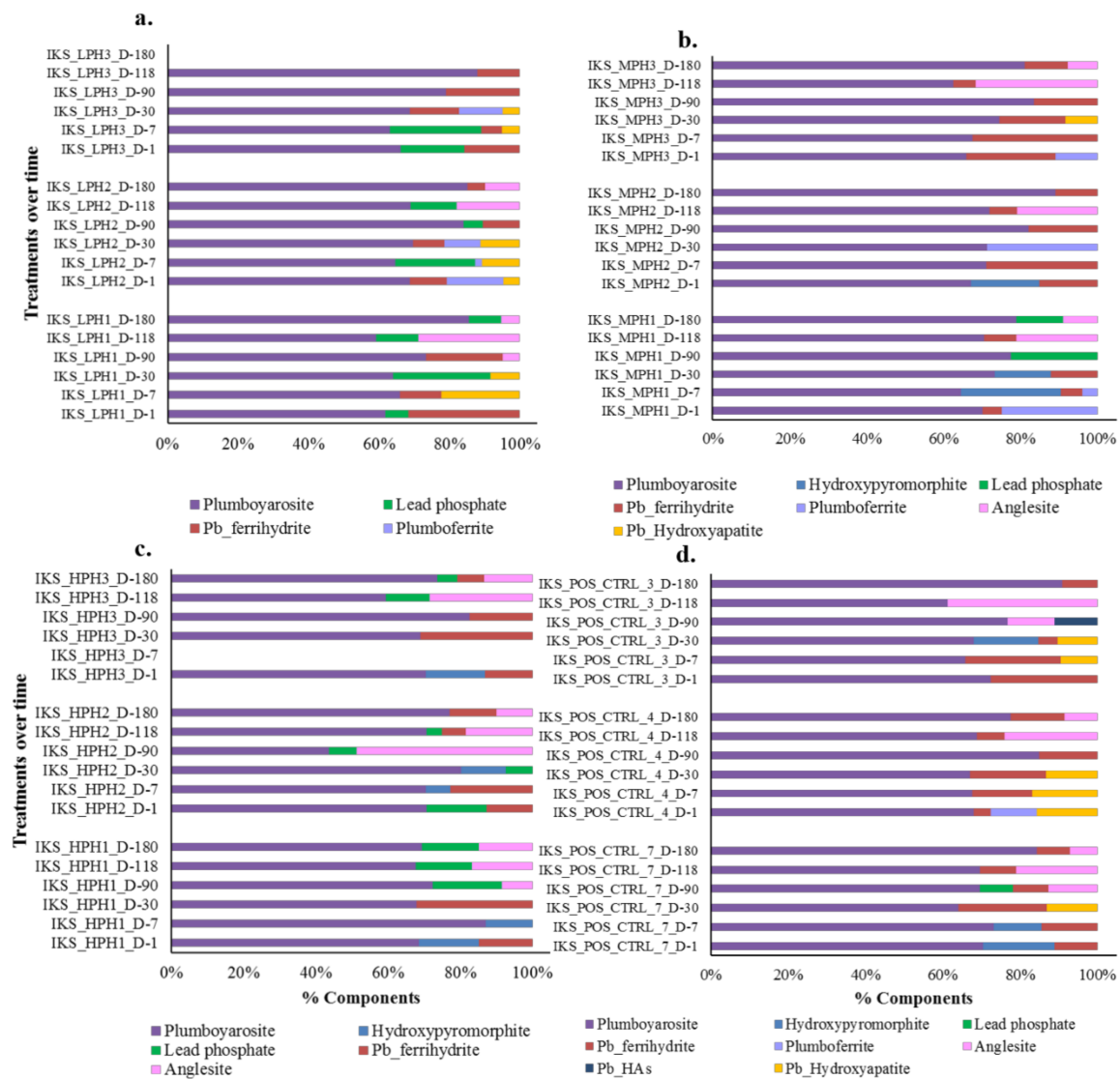


Figure 1. Bar chart represents the bulk Pb-X-ray absorption spectroscopy (XAS) results obtained via statistical analyses; principal component analysis (PCA), and linear combination fitting (LCF) results showing % components of Pb minerals in (a) Low P-amended (1%); (b) Medium P-amended (5%); (c) High P-amended (10%); (d) Non-amended positive control for IKS at pH_{PZC} (pH 4), $>pH_{PZC}$ (pH 7), and $<pH_{PZC}$ (pH 3) for 1-, 7-, 30-, 90-, 118-, and 180-day of incubation. IKS in the label represents IKJ 583, “L” stands for low P-amendment, “M” for medium P-amendment, and “H” for high P-amendment. “PH1” in the samples label represents $>pH_{PZC}$, “PH2” represents pH_{PZC} , and “PH3” represents $<pH_{PZC}$. “POS_CTRL” stands for positive control. “D” represents for the days of incubation. “HAs” in the label represents humic acids.

Table 2. Treatment effect ratio (TER) for bioaccessible lead measurement at pH 1.5 and pH 2.5 for IKS (IKJ 583).

Lead	pH 1.5						pH 2.5					
	Day 1	Day 7	Day 30	Day 90	Day 118	Day 180	Day 1	Day 7	Day 30	Day 90	Day 118	Day 180
Treatment	TER	TER	TER	TER	TER	TER	TER	TER	TER	TER	TER	TER
IKS_LPH1 > PZC (7.0)	0.34	0.29	0.39	0.49	0.57	0.71	0.17	0.21	0.25	0.35	0.34	0.37
IKS_LPH2 PZC (4.0)	0.72	0.79	0.97	2.38	2.26	0.99	0.44	0.49	0.68	0.69	1.76	0.53
IKS_LPH3 < PZC (3.0)	0.86	2.17	1.96	1.55	1.46	1.13	0.65	0.59	1.75	0.7	1.69	0.41
IKS_MPH1 > PZC (7.0)	0.35	0.34	0.38	0.41	0.41	0.72	0.17	0.19	0.18	0.16	0.16	0.48
IKS_MPH2 PZC (4.0)	0.91	0.94	1.08	2.15	2.66	1.58	0.58	0.76	0.62	1.39	2.26	0.53
IKS_MPH3 < PZC (3.0)	1.04	2.63	2.25	1.74	1.65	2.00	1.00	0.94	1.74	1.48	1.5	1.14
IKS_HPH1 > PZC (7.0)	0.38	0.40	0.37	0.39	0.40	0.56	0.17	0.21	0.23	0.24	0.19	0.52
IKS_HPH2 PZC (4.0)	1.05	1.04	1.19	2.66	2.49	1.74	0.60	0.75	0.46	1.02	1.44	0.85
IKS_HPH3 < PZC (3.0)	1.16	3.28	2.11	3.60	1.82	1.80	1.06	0.74	1.53	2.46	1.82	0.46

Arsenic	pH 1.5						pH 2.5					
	Day 1	Day 7	Day 30	Day 90	Day 118	Day 180	Day 1	Day 7	Day 30	Day 90	Day 118	Day 180
Treatment	TER	TER	TER	TER	TER	TER	TER	TER	TER	TER	TER	TER
IKS_LPH1 > PZC (7.0)	1.51	1.65	1.80	1.58	1.84	2.07	3.68	4.53	4.93	2.86	3.95	4.65
IKS_LPH2 PZC (4.0)	1.14	1.25	1.50	1.14	1.34	1.57	2.22	2.48	2.88	1.73	2.99	2.48
IKS_LPH3 < PZC (3.0)	0.93	0.91	1.08	1.10	1.13	1.35	2.01	2.09	2.18	1.94	2.20	2.01
IKS_MPH1 > PZC (7.0)	0.70	1.98	2.45	1.84	1.34	2.28	5.34	7.92	10.89	5.19	8.29	8.01
IKS_MPH2 PZC (4.0)	0.93	0.93	0.94	0.50	1.04	0.95	1.53	1.42	1.30	1.06	1.73	1.23
IKS_MPH3 < PZC (3.0)	0.75	0.64	0.57	0.60	0.63	0.62	0.93	1.11	0.86	0.79	0.94	0.85
IKS_HPH1 > PZC (7.0)	1.52	1.79	2.22	1.83	2.16	2.31	4.94	7.14	9.66	5.09	7.50	8.55
IKS_HPH2 PZC (4.0)	0.81	0.80	0.69	0.79	0.74	0.69	2.01	1.13	0.86	0.76	1.22	0.89
IKS_HPH3 < PZC (3.0)	0.68	0.55	0.41	0.46	0.46	0.41	1.35	0.84	0.56	0.58	0.73	0.68

Treatment effect ratio (TER) represents the bioaccessibility in amended soil divided by bioaccessibility in the untreated soil at that particular pH. IKS in the label represents IKJ 583, “L” stands for low P-amendment, “M” for medium P-amendment, and “H” for high P-amendment. “PH1” in the samples label represents >pH_{PZC} (pH 7) “PH2” represents pH_{PZC} (pH 4), and “PH3” represents <pH_{PZC} (pH 3).

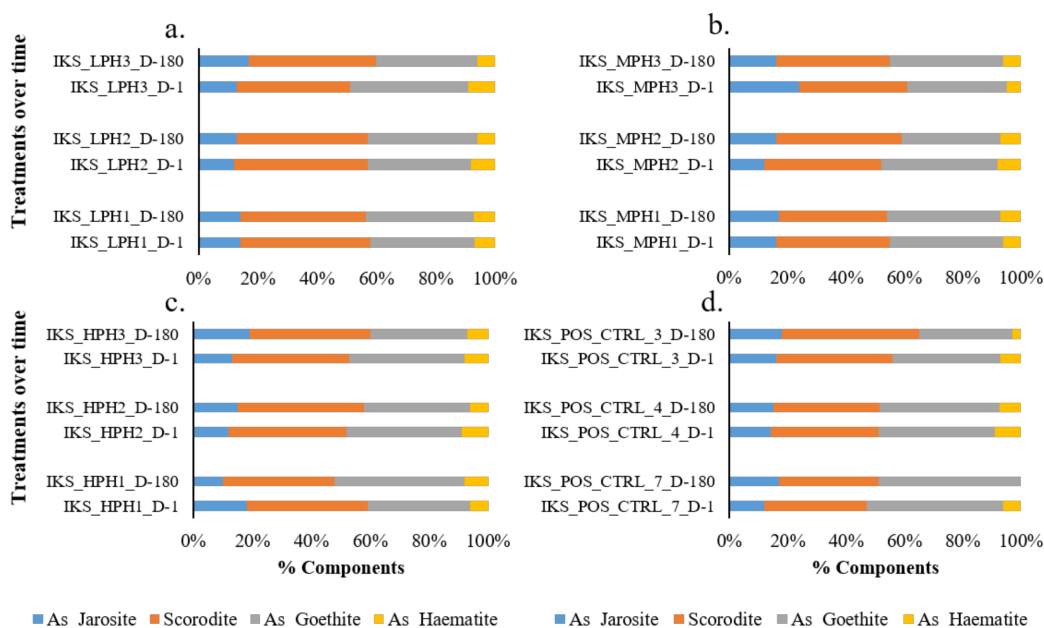


Figure 2. Bar chart represents the bulk As-XAS results obtained via statistical analyses; principal component analysis (PCA), and linear combination fitting (LCF) showing % components of Pb-minerals in (a) Low P-amended (1%); (b) Medium P-amended (5%); (c) High P-amended (10%); (d) Non-amended positive control for IKJ 583 at pH_{PZC} (pH 4), >pH_{PZC} (pH 7), and <pH_{PZC} (pH 3) for 1- and 180-day of incubation. IKS in the label represents IKJ 583, “L” stands for low P-amendment, “M” for medium P-amendment, and “H” for high P-amendment. “PH1” in the samples label represents >pH_{PZC} (pH 7), “PH2” represents pH_{PZC} (pH 4), and “PH3” represents <pH_{PZC} (pH 3). “POS_CTRL” stands for positive control. “D” represents for the days of incubation.

3.3.2. BO

The ICP-OES analysis conducted on the effluent samples of BO indicated that total soluble Pb was lowest with high P-amendment at higher pH ($>pH_{PZC}$) similar to IKS (Table S3). Nonetheless, total dissolved As concentrations were lowest in the low P-amended treatments set at $>pH_{PZC}$, indicating pH effect to be more predominant upon low P-application in reducing the total dissolved As concentration in effluent samples. This observation could be self-evident as a result of the known effect of competitive adsorption mechanism between arsenate and phosphate with high P-amendment, as described earlier.

Lead-XAS data analysis on post P-amended samples at different pHs indicated Pb adsorbed to ferrihydrite (27% to 37%) and Pb bound to organic matter (15% to 63%) as the primary dominant minerals [26] which are commonly observed in soil with high Fe oxides and high organic matter [48]. Adsorption of organic matter, especially humic substances, onto a mineral surface alters its physical and chemical properties, influencing the sorption and desorption processes of ions like phosphates and heavy metals. In addition, organic coatings on pyromorphite crystals seeds are also known to inhibit further pyromorphite formation [49,50]. These could be the reasons for observing low pyromorphite formation in all the treatment combinations of BO regardless of the different rate of P-applications. However, pyromorphite formation was slightly enhanced with high P-amendment (23%) (Figure 3). This reduced phosphate fixation could be attributed to the competitive sorption of fulvic polyanions and their favorable sorption onto mineral particles [49]. The data obtained from other tested soils with three replicates showed higher consistency which indicates that there may not have been any limitations on the conclusion derived from only one replicate used in BO. However, long-term incubation for BO might derive more information on the trend of Pb- and As-bioaccessibility results over time.

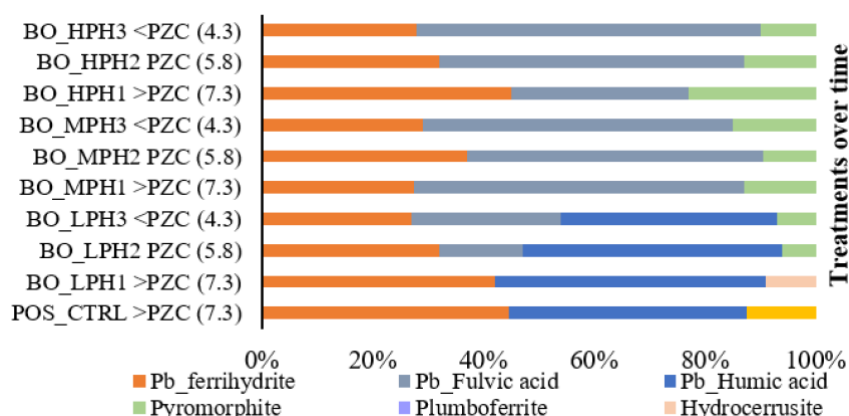


Figure 3. Bar chart represents the bulk Pb-XAS results obtained via statistical analyses; principal component analysis (PCA), and linear combination fitting (LCF) showing % components of Pb-minerals in low P-amended (1%), medium P-amended (5%), high P-amended (10%) and non-amended positive control for BO at pH_{PZC} (pH 5.8), $>pH_{PZC}$ (pH 7.3), and $<pH_{PZC}$ (pH 4.3) for 37-day of incubation. “L” in the sample labels stands for low P-amendment, “M” for medium P-amendment, and “H” for high P-amendment. “PH1” in the samples label represents $>pH_{PZC}$, “PH2” represents pH_{PZC} , and “PH3” represents $<pH_{PZC}$. “POS_CTRL” stands for positive control.

The values for Pb TERs estimations in BO were <1 , falling in the low to median range of 0.53 to 0.75 at pH 2.5 and 0.66 to 0.79 at pH 1.5 (Table 3). The presence of Pb sorbed to ferrihydrite in BO might have contributed significantly to the bioaccessible Pb pool, possibly because of dissolution and re-precipitation during IVBA extraction procedure [51–53].

Table 3. Treatment effect ratio (TER) for bioaccessible lead measurement at pH 1.5 and pH 2.5 for BO.

Lead	pH 1.5	pH 2.5
	Day 37	
Treatment	TER	TER
BO_LPH1 > PZC (7.3)	0.79	0.75
BO_LPH2 PZC (5.8)	0.79	0.75
BO_LPH3 < PZC (4.3)	0.77	0.71
BO_MPH1 > PZC (7.3)	0.77	0.72
BO_MPH2 PZC (5.8)	0.65	0.60
BO_MPH3 < PZC (4.3)	0.83	0.69
BO_HPH1 > PZC (7.3)	0.78	0.71
BO_HPH2 PZC (5.8)	0.66	0.60
BO_HPH3 < PZC (4.3)	0.82	0.53
Arsenic		
BO_LPH1 > PZC (7.3)	1.12	1.12
BO_LPH2 PZC (5.8)	1.35	1.53
BO_LPH3 < PZC (4.3)	0.86	0.82
BO_MPH1 > PZC (7.3)	0.96	0.87
BO_MPH2 PZC (5.8)	1.11	1.12
BO_MPH3 < PZC (4.3)	0.72	0.60
BO_HPH1 > PZC (7.3)	0.90	0.75
BO_HPH2 PZC (5.8)	0.94	0.84
BO_HPH3 < PZC (4.3)	0.69	0.42

Treatment effect ratio (TER) represents the bioaccessibility in amended soil divided by bioaccessibility in the untreated soil at that particular pH. BO in the label represents Barber orchard soil, “L” stands for low P-amendment, “M” for medium P-amendment, and “H” for high P-amendment. “PH1” in the samples label represents $>pH_{PZC}$ (pH 7.3) “PH2” represents pH_{PZC} (pH 5.8), and “PH3” represents $<pH_{PZC}$ (pH 4.3).

Arsenic speciation in post-amended BO indicated As(V) sorbed to goethite (11% to 43%), As sorbed to birnessite (12% to 49%), arseniosiderite (19% to 37%), and Pb-arsenate pesticide (12% to 30%) (Figure 4). Considering an initial As mineralogy, competitive retention of As between Fe and Mn oxides was observed as arsenic sorbed to birnessite was decreased and redistributed to goethite. This increased preferential partition of As(V) from birnessite to goethite could be a result of higher adsorption affinity of As with goethite compared to birnessite [54]. The presence of Pb-arsenate pesticide ($PbHAsO_4$) confirms its established properties as relatively insoluble and persistent. Approximately 17% to 37% of arseniosiderite ($Ca_2Fe_3^{3+}O_2(AsO_4)_3 \cdot 3H_2O$) was formed in the post-amended BO at pH_{PZC} . Literature is limited on understanding the conditions promoting arseniosiderite formation and dissolution.

In the current study, formation of arseniosiderite displayed the influence of adsorption and precipitation reaction in Fe-rich aqueous environment favored with the Ca/As + Fe + Ca ratio of 0.13 (required: 0.1) and the pH of slightly acidic to alkaline (4.3 to 7.3) as minimum requirements for arseniosiderite formation [55]. The TERs estimations for As in BO were usually high, yet values of 0.42 (pH 2.5) and 0.69 (pH 1.5) were observed in HPH3 at pH 4.3 (Table 3). Among oxides of Fe/Al/Mn, Fe-oxide minerals, such as hydrous ferric oxide (HFO), goethite, and hematite, are considered to be the most important sinks for As under-oxidized conditions [56,57]; still, the extent of adsorption depended upon the initial concentration, pH, and competing ions present in solution [58]. High organic carbon (~7.2%) in BO may also have resulted in increased As TERs estimations.

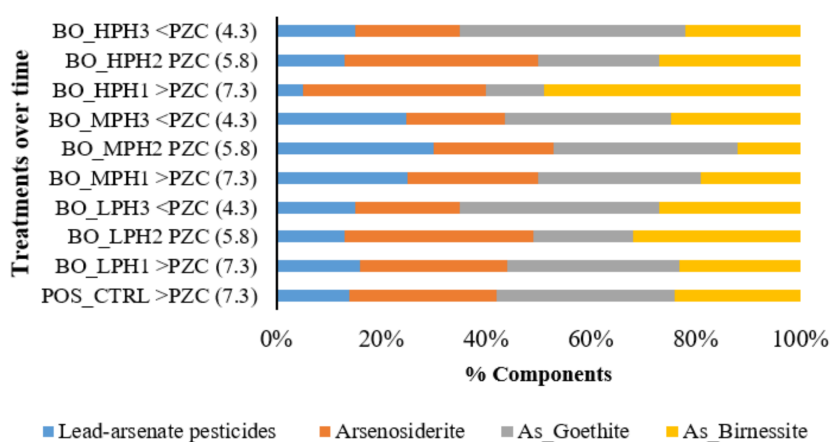


Figure 4. Bar chart represents the bulk As-XAS results obtained via statistical analyses; principal component analysis (PCA), and linear combination fitting (LCF) showing % components of Pb-minerals in low P-amended (1%), medium P-amended (5%), high P-amended (10%) and non-amended positive control for BO at pH_{PZC} (pH 5.8), $>pH_{PZC}$ (pH 7.3), and $<pH_{PZC}$ (pH 4.3) for 37-day of incubation. “L” in the sample labels stands for low P-amendment, “M” for medium P-amendment, and “H” for high P-amendment.

3.3.3. NW

Total dissolved Pb concentration in NW indicated no noticeable difference with variable rate of P-amendment at different pHs. However, slightly enhanced soluble Pb was detected at $<pH_{PZC}$. A similar trend was observed with non-amended POS_CTRL indicating Pb was less soluble especially at circumneutral pH. Total dissolved As in NW displayed a similar trend as IKS where soluble As was least detected at $>pH_{PZC}$ and with low P-amendment (Table S4).

Lead mineralogy in post-amended treatments of NW (Figure 5) showed slight alterations as Pb sorbed to humic acids and Pb sorbed to ferrihydrite were both identified as primary dominant phases (~20% to 80%). The other minor Pb-minerals included lead phosphates, magnetoplumbite, Pb sorbed to hydroxyapatite, cerussite, and anglesite, among which Pb-phosphates were frequently observed at higher pH which was supported by reduction in phosphate (anions) measurements at $>pH_{PZC}$ (Table S6). However, no particular trend in Pb-phosphate formation was observed. Among the two dominant minerals, Pb sorbed to ferrihydrite decreased (from 90% to 12%), whereas Pb sorbed to humic acids showed an increasing trend (12% to 90%) from day-1 to day-180 of incubation (Figure 5). In NW, redistribution of Pb from mineral surfaces to organic matter at higher pH ($>pH_{PZC}$ of 8) was likely related to the strong affinity of Pb(II) to partition on organic matter either via electrostatic or chemical bonds with surface functional groups which decreases with a decrease in pH, as supported by Cao et al. [5] and Wang et al. [59].

Despite fairly similar mineralogy, across the treatments, TERs estimations for Pb bioaccessibility measurements were 0.50 to 0.72 at pH 2.5, and ~0.6 at pH 1.5 in the treatment set at $>pH_{PZC}$ with both medium and high P-amendments, whereas the highest Pb TER estimation stayed between 1.19 to 1.33 with low P-amendment at higher pHs in NW (Table 4).

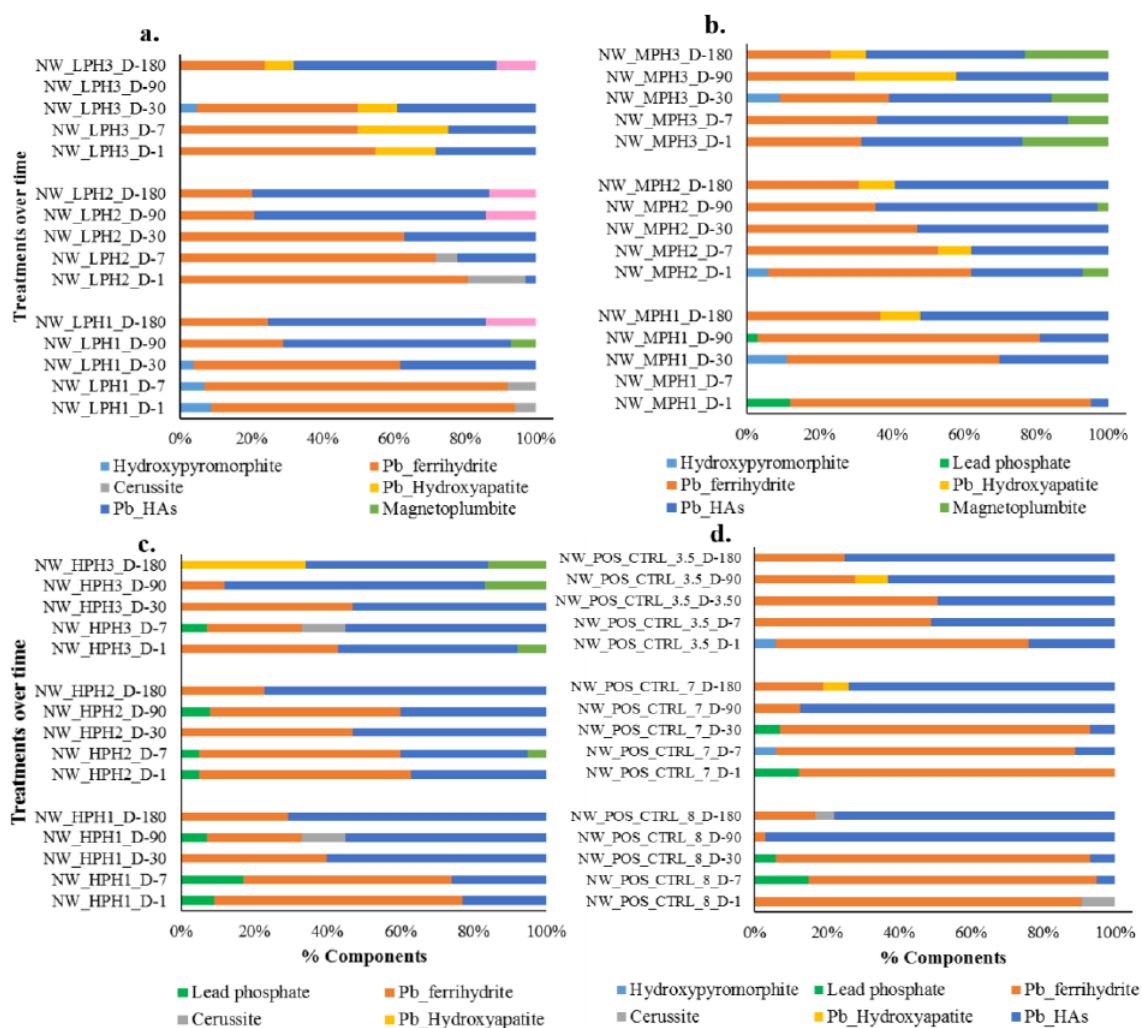


Figure 5. Bar chart represents the bulk Pb-XAS results obtained via statistical analyses; principal component analysis (PCA), and linear combination fitting (LCF) showing % components of Pb-minerals in (a) Low P-amended (1%) (b) Medium P-amended (5%), (c) High P-amended (10%) and (d) non-amended positive control for NW at pH_{PZC} (pH 7), $>pH_{PZC}$ (pH 8), and $<pH_{PZC}$ (pH 3.5) at 1-, 7-, 30-, 90-, and 180-day of incubation. “L” in the sample labels stands for low P-amendment, “M” for medium P-amendment, and “H” for high P-amendment. “PH1” in the samples label represents $>pH_{PZC}$, “PH2” represents pH_{PZC} , and “PH3” represents $<pH_{PZC}$. “POS_CTRL” stands for positive control. “D” represents for the days of incubation.

Arsenic speciation in NW with very low As concentration (19 mg kg^{-1}) (Table 1) indicated the presence of As(V)_jarosite and scorodite as the predominant minerals with As(V) sorbed to birnessite, As(V) sorbed to goethite, As(V) sorbed to ferrihydrite, loellingite, and arseniosiderite as the minor minerals. While mineralogical composition remained almost similar, there were increments in % component of As(V)_jarosite (from 18% to 48%) and scorodite (from 13% to 55%) in all the treatment combinations compared to As-speciation in the starting NW used in this study. Overall, TER_{As} values were lower for all high P-amended samples at all pHs; however, the smallest TER value (0.42) was estimated at $>pH_{PZC}$ which could be a result of the presence of more stable As minerals such as As(V)_jarosite and scorodite as well as the possible formation of insoluble calcium arsenate at higher pH (Figure 6). This speculation can also be supported by soluble Ca data provided in Table S4. Arsenic incorporation in the jarosite structure could have potentially increased the stabilization of the jarosite structure and decreased its solubility, as reported by Baron and Palmer [60]. In addition, scorodite is

known as one of the least bioaccessible (0.13%) with (log K_{sp} of -25.8) arsenate phases reported in mining-impacted soils [61].

Table 4. Treatment effect ratio (TER) for bioaccessible lead measurement at pH 1.5 and pH 2.5 for NW.

Lead	pH 1.5					pH 2.5				
	Day 1	Day 7	Day 30	Day 90	Day 180	Day 1	Day 7	Day 30	Day 90	Day 180
NW_LPH1 > PZC (8.0)	1.01	0.93	0.91	0.96	0.97	0.91	0.89	0.97	0.92	1.00
NW_LPH2 PZC (7.0)	1.02	0.92	0.89	0.92	0.99	0.95	0.85	0.89	0.84	0.95
NW_LPH3 < PZC (3.5)	0.95	0.91	1.11	1.17	1.19	0.97	1.05	1.10	1.24	1.33
NW_MPH1 > PZC (8.0)	0.94	0.90	0.86	0.93	0.97	0.71	0.70	0.80	0.74	0.81
NW_MPH2 PZC (7.0)	0.98	0.88	0.85	0.89	0.93	0.75	0.63	0.72	0.66	0.79
NW_MPH3 < PZC (3.5)	0.94	0.95	1.12	1.14	1.22	0.98	1.00	1.05	1.08	1.21
NW_HPH1 > PZC (8.0)	0.94	0.93	0.85	0.88	0.93	0.69	0.67	0.75	0.64	0.69
NW_HPH2 PZC (7.0)	0.97	0.86	0.86	0.84	0.93	0.67	0.59	0.67	0.64	0.69
NW_HPH3 < PZC (3.5)	0.96	0.93	1.12	1.09	1.11	0.93	0.95	0.94	0.95	1.07

Arsenic	pH 1.5					pH 2.5				
	Day 1	Day 7	Day 30	Day 90	Day 180	Day 1	Day 7	Day 30	Day 90	Day 180
Treatment	TER	TER	TER	TER	TER	TER	TER	TER	TER	TER
NW_LPH1 > PZC (8.0)	1.16	1.06	1.11	1.15	1.18	1.09	1.09	1.21	1.27	1.22
NW_LPH2 PZC (7.0)	1.09	1.02	0.97	1.03	1.55	1.12	1.05	1.14	1.05	1.01
NW_LPH3 < PZC (3.5)	0.88	0.84	0.98	1.00	1.06	0.91	0.95	0.86	1.04	1.08
NW_MPH1 > PZC (8.0)	1.04	1.04	1.03	1.23	1.13	0.95	1.01	1.09	1.28	1.19
NW_MPH2 PZC (7.0)	0.92	0.92	0.96	1.07	1.02	0.93	1.32	0.96	1.01	0.81
NW_MPH3 < PZC (3.5)	0.75	0.76	0.75	0.74	0.75	0.89	0.82	0.73	0.70	0.76
NW_HPH1 > PZC (8.0)	0.79	0.71	0.61	0.55	0.54	0.73	0.64	0.50	0.43	0.42
NW_HPH2 PZC (7.0)	0.76	0.63	0.60	0.56	0.82	0.72	0.90	0.52	0.47	0.45
NW_HPH3 < PZC (3.5)	0.64	0.69	0.65	0.60	0.62	0.72	0.73	0.59	0.50	0.59

Treatment effect ratio (TER) represents the bioaccessibility in amended soil divided by bioaccessibility in the untreated soil at that particular pH. NW in the label represents Northwestern soils, "L" stands for low P-amendment, "M" for medium P-amendment, and "H" for high P-amendment. "PH1" in the samples label represents $>pH_{PZC}$ (pH 8) "PH2" represents pH_{PZC} (pH 7), and "PH3" represents $<pH_{PZC}$ (pH 3.5).

Overall, the current study indicated very slight Pb and As mineralogical changes with different rates of P-application in combination with pH set at, above, and below PZC. No significant role of PZC was observed in pyromorphite formation. While the pH–PZC relationship may not have had a significant impact on Pb and As mineralogy, there were significant differences in the measured TER values for As and Pb after P-amendment. A one-way ANOVA was conducted on the individual factors in the study which would have influenced the change in Pb and As bioaccessibility (pH–PZC relationship, P-application, and time). Across the three, the only significant factor contributing to a change in the TER for Pb or As was the pH–PZC relationship (ANOVA_{TER-Pb}, $F = 26.6$, p -value < 0.001 and ANOVA_{TER-As}, $F = 20.79$, p -value < 0.001). Additional factors, P-application, and time were not significant. To further evaluate potential interactions between the pH–PZC relationship and P-application or between the pH–PZC relationship and time, a two-way ANOVA was conducted. Results from the analysis did not indicate there were any significant interactions between the factors. Posthoc Tukey's means comparisons for the different pH–PZC relationships revealed that the TER_{Pb} values for all three means were statistically different from one other with the pH>PZC having the minimum value (Figure 7). The Tukey's means comparison for TER_{As} value indicated no difference between the mean TER_{As} value for pH = PZC or pH > PZC. However, the TER_{As} value was significantly lower when the pH < PZC after P-amendment.

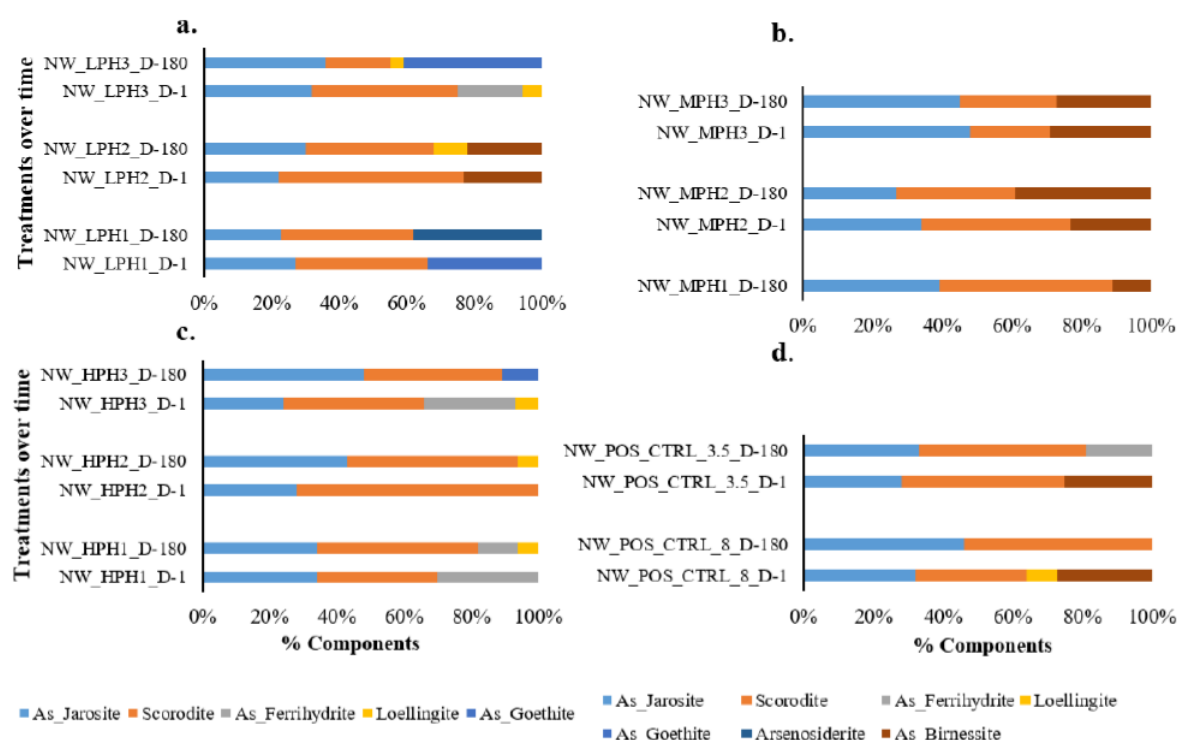


Figure 6. Bar chart represents the bulk As-XAS results obtained via statistical analyses; principal component analysis (PCA), and linear combination fitting (LCF) showing % components of Pb-minerals in (a) Low P-amended (1%); (b) Medium P-amended (5%); (c) High P-amended (10%) and (d) non-amended positive control for NW at pH_{PZC} (pH 4), $>pH_{PZC}$ (pH 7), and $<pH_{PZC}$ (pH 3) for 1- and 180-day of incubation. “D” represents for the days of incubation.

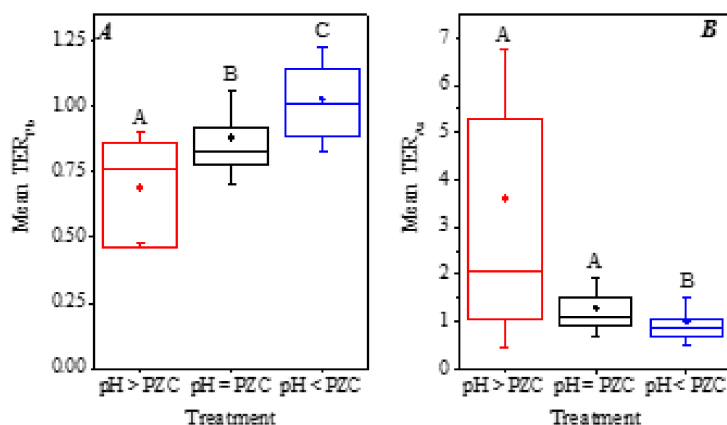


Figure 7. Box and whisker plots for the mean TER values for Pb and As as a function of the pH–PZC relationship. The mean is represented by the symbol in each box and whisker plot. The box ends represent the 25th and 75th percentiles, while the middle line is equal to the median value. The whiskers are equal to one standard deviation from the mean value (symbol). (A) Mean TER_{Pb} values; (B) Mean TER_{As} values.

The total number of TER measurements for each soil type based on each treatment factor (pH– PZC relationship, P-loading, and time) was 9, 45, and 54 for BO, NW, and IKS, respectively. As a result of an unbalanced design with respect to the number of TER measurements collected for each soil type, it was not possible to determine if the soil type was a significant factor related to the changes

in bioaccessibility after P-amendment. However, a visual comparison of the mean TER_{Pb} and TER_{As} values as a function of soil type indicated that there was a slight difference among the TER_{Pb} value calculated for all of the pH–PZC conditions evaluated (Supplemental Figure S2). The range of values obtained for the IKS soil showed a much higher degree of variability compared to the BO and NW soils. Further analysis of the range of TER values for Pb and As as a function of the pH–PZC relationship were analyzed to assess how soil properties may influence the measured TER (Figure 8). The data presented in Figure 8 would indicate that soil type is an important factor along with the pH–PZC relationship when considering changes in bioaccessible As and Pb in P amended soils. As previously noted, the range of TER values for each pH–PZC for the IKS was much greater than the range of values for the other two soils (Figure S2) and the response of the measured TER value between different pH–PZC relationships; As and Pb was greatest for IKS. IKS differed from the other two soils in the amount of Fe present (14% by weight), S (8.5% by weight), and the large concentration of As (3850 mg kg^{-1}). It is likely the large TER_{As} value measured for IKS, when the pH was less than the PZC (pH 3), was a result of Fe mineral dissolution because the majority of As species present in the soil were associated with scorodite and As-adsorbed to iron oxides (Figure 2 and Table S2). Even the dissolution of a small amount of Fe could have a large impact on the bioaccessible fraction of As. The reduced TER_{Pb} value for IKS compared to BO and NW at $>pH_{PZC}$ was likely related to the Pb speciation. IKS Pb speciation was dominated by a crystalline form of Pb, plumbojarosite, making it less likely to be released during the in vitro extraction compared to sorbed Pb species which were dominant in the NW and BO. As the pH decreased toward and below the PZC (pH 4 and 3) in IKS, the solubility of jarosite minerals increased, thus allowing for increased extraction of Pb due to dissolution at the mineral surface.

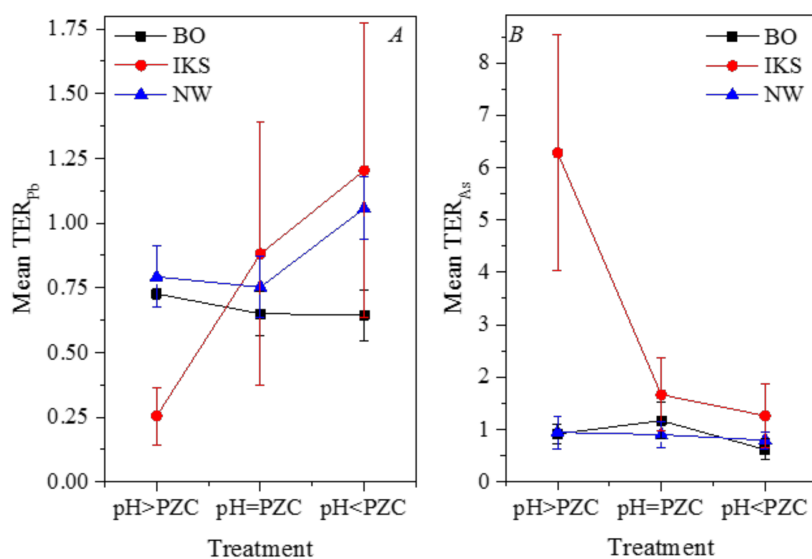


Figure 8. Mean TER values for the three pH–PZC relationships for individual soil types tested. The error bars represent one standard deviation from the mean value (symbol). (A) Mean TER_{Pb} values; (B) Mean TER_{As} values.

4. Conclusions

Phosphate amendments have been recommended for mitigating the risk associated with Pb by forming highly insoluble Pb species such as pyromorphite. The formation of insoluble pyromorphite in P-amended soils have been considerably successful in lab-based studies, but limited success has been found in field studies. Focused studies to investigate mechanisms to promote pyromorphite formation in field studies are needed to facilitate utilization of this technology. This study proposed to examine the role of PZC in combination with different rates of P-applications in pyromorphite

formation and bioaccessibility of Pb and As in phosphate-amended soils. Overall, the results obtained from the current study indicated that there was no significant effect of PZC on pyromorphite formation in P-amended soils; however, the TER for Pb bioaccessibility appeared to be lower when $\text{pH} > \text{PZC}$. In contrast, the As TER was lower when $\text{pH} < \text{PZC}$ in all three tested soils. In particular, the reduced TER_{Pb} value for IKS compared to BO and NW when $\text{pH} > \text{PZC}$, was likely related to the Pb speciation dominated by a crystalline form of Pb, plumbojarosite. This made it less likely to be released during the *in vitro* extraction compared to sorbed Pb species which were dominant in NW and BO. In contrast, the large TER_{As} value measured for IKS (14% Fe, 8.5% S, and 3850 mg kg⁻¹ As), when $\text{pH} < \text{PZC}$ was a result of Fe-mineral dissolution as the majority of As species present in the soil were associated with scorodite and As-adsorbed to iron oxides. High organic matter content in BO (~7.2%) was likely an inhibitor of pyromorphite formation due to occlusion; nevertheless, high Fe and Mn content and associated more stable minerals present in the tested soils might have been responsible in reducing the bioaccessibility of both Pb and As over time. Higher Ca content in NW may have resulted in the formation of insoluble calcium phosphates at $\text{pH} > \text{PZC}$ due to its adsorption site competition with Pb thereby inhibiting pyromorphite formations. However, the TER for Pb in NW was reduced at $\text{pH} > \text{PZC}$ attributable to the redistribution of lead to organics bound in combination with high pH. Overall, lower TER values for As was observed for high P-amended NW samples; however, the smallest TER for As was estimated for the high P-amended samples at $>\text{pH}_{\text{PZC}}$ which was likely a result of the more stable As mineralogy as well as possible calcium arsenate formation at high pH.

However, caution must be taken for phosphate-amended soils in which competitive reactions may enhance contaminant mobility and bioavailability, such as the case of As in this study. The lack of conversion of soil Pb to pyromorphite may be attributed to several reasons, possibly a result of the presence of highly stable minerals, such as plumbojarosite, which limits soluble Pb availability to react with phosphates. The speculations discussed above are also supported by the data obtained from a similar study conducted by using Pb–acetate spiked soils (3000 mg Pb per kg of soil, equilibrated for two weeks under 40% field capacity and room temperature). The TER data obtained over 30-day of incubation (Table S8) indicated lower values at higher pH which was similar to other tested soils in this study. However, Pb-XAS data indicated increased pyromorphite formation (Figure 1) at higher pH. The newly spiked soil used in this study lacked highly stable minerals; instead, they were mostly dominated by sorbed Pb phases. The presence of Pb species with higher dissolution rates enhanced pyromorphite formation in the newly spiked soils. Additional aged soils need to be tested in order to confirm the role of PZC on pyromorphite formations in P-amended soils.

Supplementary Materials: There are eight supplementary tables and three supplementary figures provided in this document. The following are available online at <http://www.mdpi.com/2571-8789/2/2/22/s1>. Table S1: Recovery percentage for QA/QC samples during a) lead and arsenic IVBA extraction procedure (EPA Method 1340), and b) EPA 3051A acid digestion. Table S2: Total dissolved elements measurement from effluent samples collected from IKJ 583 at 1-, 7-, 30, 90-, and 180-day of incubation using ICP-OES. Table S3: Total dissolved elements measurement in effluent samples collected from BO at 37-day of incubation using ICP-OES. Table S4: Total dissolved elements measurement in effluent samples collected from NW at 1-, 7-, 30, 90-, and 180-day of incubation using ICP-OES. Table S5: Sulfate and phosphate measurements in IKJ 583. Table S6: Sulfate and phosphate measurements in NW. Table S7: Sulfate and phosphate measurements in BO. Table S8: Treatment effect ratio (TER) for bioaccessible lead measurement at pH 1.5 and pH 2.5 for artificially spiked soil (CS). Figure S1: Bar chart represents the bulk Pb-XAS results obtained via statistical analyses; principal component analysis (PCA), and linear combination fitting (LCF) results showing % components of Pb-minerals in a) Medium P-amended (5%) of artificially lead-spiked soil $>\text{pHPZC}$ (pH 7.5, 8.5), and $<\text{pHPZC}$ (pH 3.5) for 1-, 7-, 30-day of incubation. CS in the label represents clean soil spiked with lead, “M” stands for medium P-amendment. “PH1” and “PH2” in the samples label represents $>\text{pHPZC}$, and “PH3” represents $<\text{pHPZC}$. “POS_CTRL” stands for positive control. Figure S2: Box and whisker plots for the mean TER values for Pb and As as a function of soil type. The mean is represented by the symbol in each box and whisker plot. The box ends represent the 25th and 75th percentiles, while the middle line is equal to the median value. The whiskers are equal to one standard deviation from the mean value (symbol). (A) Mean TER_{Pb} values, (B) Mean TER_{As} values. Figure S3: Dissolved Fe concentration for the IKS soil for each of the three pH-PZC relationships at the P-application rate of 1%.

Acknowledgments: The US EPA funded and managed the research described here. It has been subjected to agency review and approved for publication. Mention of trade names or commercial products does not constitute endorsement or recommendation for use. We acknowledge the support of the Materials Research Collaborative

Access Team (MRCAT) (Sector 10-ID, and 10-BM). The MRCAT operations are supported by the Department of Energy and the MRCAT member institutions. This research used resources of the Advanced Photon Source, a US Department of Energy (DOE) Office of Science User Facility operated for the DOE Office of Science by Argonne National Laboratory under contract no. DE-AC02-06CH11357. We are also thankful to Jennifer Goetz and Aaron Betts for their help during the initial phase of experiment setup.

Author Contributions: R.R.K. conceived, designed, and performed the experiments with the support of K.G.S., and wrote the paper with input from K.G.S. and M.N.; K.G.S. assisted in collecting the XAS data at APS; T.P.L. assisted to conduct the statistical analysis and review the manuscript.

Conflicts of Interest: The authors declare no conflict of interest.

References

1. Hettiarachchi, G.M.; Pierzynski, G.M. Soil lead bioavailability and in situ remediation of lead-contaminated soils: A review. *Environ. Prog. Sustain. Energy* **2004**, *23*, 78–93. [[CrossRef](#)]
2. Porter, S.K.; Scheckel, K.G.; Impellitteri, C.A.; Ryan, J.A. Toxic metals in the environment: Thermodynamic considerations for possible immobilization strategies for Pb, Cd, As, and Hg. *Crit. Rev. Environ. Sci. Technol.* **2004**, *34*, 495–604. [[CrossRef](#)]
3. Scheckel, K.G.; Ryan, J.A. Spectroscopic speciation and quantification of lead in phosphate-amended soils. *J. Environ. Qual.* **2004**, *33*, 1288–1295. [[CrossRef](#)] [[PubMed](#)]
4. US EPA. *Q's and A's Fact Sheet on MTBE in Water*; Office of Water: Washington, DC, USA, 1996.
5. Cao, X.; Wahbi, A.; Ma, L.; Li, B.; Yang, Y. Immobilization of Zn, Cu, and Pb in contaminated soils using phosphate rock and phosphoric acid. *J. Hazard. Mater.* **2009**, *164*, 555–564. [[CrossRef](#)] [[PubMed](#)]
6. Hettiarachchi, G.M.; Pierzynski, G.M.; Ransom, M.D. In situ stabilization of soil lead using phosphorus and manganese oxide. *Environ. Sci. Technol.* **2000**, *34*, 4614–4619. [[CrossRef](#)]
7. Ma, Q.Y.; Traina, S.J.; Logan, T.J.; Ryan, J.A. In situ lead immobilization by apatite. *Environ. Sci. Technol.* **1993**, *27*, 1803–1810. [[CrossRef](#)]
8. Nriagu, J.O. Lead orthophosphates—IV Formation and stability in the environment. *Geochim. Cosmochim. Acta* **1974**, *38*, 887–898. [[CrossRef](#)]
9. Scheckel, K.G.; Diamond, G.L.; Burgess, M.F.; Klotzbach, J.M.; Maddaloni, M.; Miller, B.W.; Partridge, C.R.; Serda, S.M. Amending soils with phosphate as means to mitigate soil lead hazard: A critical review of the state of the science. *J. Toxicol. Environ. Health* **2013**, *16*, 337–380. [[CrossRef](#)] [[PubMed](#)]
10. Chappell, M.A.; Scheckel, K.G. Pyromorphite formation and stability after quick lime neutralisation in the presence of soil and clay sorbents. *Environ. Chem.* **2007**, *4*, 109–113. [[CrossRef](#)]
11. Zhang, P.; Ryan, J.A.; Yang, J. In vitro soil Pb solubility in the presence of hydroxyapatite. *Environ. Sci. Technol.* **1998**, *32*, 2763–2768. [[CrossRef](#)]
12. Butkus, M.A.; Johnson, M.C. Reevaluation of phosphate as a means of retarding lead transport from sandy firing ranges. *Soil Sediment Contam.* **2011**, *20*, 172–187. [[CrossRef](#)]
13. Debela, F.; Arocena, J.; Thring, R.; Whitcombe, T. Organic acid-induced release of lead from pyromorphite and its relevance to reclamation of Pb-contaminated soils. *Chemosphere* **2010**, *80*, 450–456. [[CrossRef](#)] [[PubMed](#)]
14. Darland, J.E.; Inskip, W.P. Effects of pH and phosphate competition on the transport of arsenate. *J. Environ. Qual.* **1997**, *26*, 1133–1139. [[CrossRef](#)]
15. Peryea, F.; Kammereck, R. Phosphate-enhanced movement of arsenic out of lead arsenate-contaminated topsoil and through uncontaminated subsoil. *Water Air Soil Pollut.* **1997**, *93*, 243–254. [[CrossRef](#)]
16. Brown, G.E., Jr.; Foster, A.L.; Ostergren, J.D. Mineral surfaces and bioavailability of heavy metals: A molecular-scale perspective. *Proc. Natl. Acad. Sci. USA* **1999**, *96*, 3388–3395. [[CrossRef](#)] [[PubMed](#)]
17. Barrow, N.; Bowden, J. A comparison of models for describing the adsorption of anions A on a variable charge mineral surface. *J. Colloid Interface Sci.* **1987**, *119*, 236–250. [[CrossRef](#)]
18. Lewis-Russ, A. Measurement of surface charge of inorganic geologic materials: Techniques and their consequences. *Adv. Agron.* **1991**, *46*, 199–243.
19. Sposito, G. On points of zero charge. *Environ. Sci. Technol.* **1998**, *32*, 2815–2819. [[CrossRef](#)]
20. Casteel, S.W.; Weis, C.P.; Henningsen, G.M.; Brattin, W.J. Estimation of relative bioavailability of lead in soil and soil-like materials using young Swine. *Environ. Health Perspect.* **2006**, *114*, 1162–1171. [[CrossRef](#)] [[PubMed](#)]

21. Scheckel, K.G.; Chaney, R.L.; Basta, N.T.; Ryan, J.A. Advances in assessing bioavailability of metal (loid) s in contaminated soils. *Adv. Agron.* **2009**, *104*, 1–52.
22. Isaure, M.; Laboudigue, A.; Manceau, A.; Sarret, G.; Tiffreau, C.; Trocellier, P.; Lamble, G.; Hazemann, J.; Chateigner, D. Quantitative Zn speciation in a contaminated dredged sediment by μ -PIXE, μ -SXRF, EXAFS spectroscopy and principal component analysis. *Geochim. Cosmochim. Acta* **2002**, *66*, 1549–1567. [[CrossRef](#)]
23. Karna, R.R.; Hettiarachchi, G.M.; Newville, M.; Sun, C.; Ma, Q. Synchrotron-based X-ray spectroscopy studies for redox-based remediation of lead, zinc, and cadmium in mine waste materials. *J. Environ. Qual.* **2016**, *45*, 1883–1893. [[CrossRef](#)] [[PubMed](#)]
24. Nachtegaal, M.; Marcus, M.; Sonke, J.; Vangronsveld, J.; Livi, K.; van Der Lelie, D.; Sparks, D. Effects of in situ remediation on the speciation and bioavailability of zinc in a smelter contaminated soil. *Geochim. Cosmochim. Acta* **2005**, *69*, 4649–4664. [[CrossRef](#)]
25. Roberts, D.R.; Scheinost, A.; Sparks, D. Zinc speciation in a smelter-contaminated soil profile using bulk and microspectroscopic techniques. *Environ. Sci. Technol.* **2002**, *36*, 1742–1750. [[CrossRef](#)] [[PubMed](#)]
26. Karna, R.R.; Noerpel, M.; Betts, A.R.; Scheckel, K.G. Lead and Arsenic Bioaccessibility and Speciation as a Function of Soil Particle Size. *J. Environ. Qual.* **2017**, *46*, 1225–1235. [[CrossRef](#)] [[PubMed](#)]
27. Schumacher, B.; Shines, K.; Burton, J.; Papp, M. Comparison of three methods for soil homogenization. *Soil Sci. Soc. Am. J.* **1990**, *54*, 1187–1190. [[CrossRef](#)]
28. US EPA. *Method 3051a: Microwave Assisted Acid Dissolution of Sediments, Sludges, Soils, and Oils*, 2nd ed.; US Government Print Office: Washington, DC, USA, 1997.
29. Sparks, D.L.; Fendorf, S.E.; Toner, C.V.; Carski, T.H. *Kinetic Methods and Measurements*; Soil Science Society of America, American Society of Agronomy: Madison, WI, USA, 1996.
30. Geebelen, W.; Adriano, D.; van der Lelie, D.; Mench, M.; Carleer, R.; Clijsters, H.; Vangronsveld, J. Selected bioavailability assays to test the efficacy of amendment-induced immobilization of lead in soils. *Plant Soil* **2003**, *249*, 217–228. [[CrossRef](#)]
31. Juhasz, A.L.; Scheckel, K.G.; Betts, A.R.; Smith, E. Predictive capabilities of in vitro assays for estimating Pb relative bioavailability in phosphate amended soils. *Environ. Sci. Technol.* **2016**, *50*, 13086–13094. [[CrossRef](#)] [[PubMed](#)]
32. Segre, C.; Leyarovska, N.; Chapman, L.; Lavender, W.; Plag, P.; King, A.; Kropf, A.; Bunker, B.; Kemner, K.; Dutta, P. The MRCAT insertion device beamline at the advanced photon source. In Proceedings of the Eleventh US National Conference Synchrotron Radiation Instrumentation, Stanford, CA, USA, 13–15 October 1999.
33. Kropf, A.; Katsoudas, J.; Chattopadhyay, S.; Shibata, T.; Lang, E.; Zyryanov, V.; Ravel, B.; McIvor, K.; Kemner, K.; Scheckel, K. The new MRCAT (Sector 10) bending magnet beamline at the advanced photon source. In Proceedings of the 10th International Conference on Radiation Instrumentation, Melbourne, Australia, 27 September–2 October 2009.
34. Davis, A.; Drexler, J.W.; Ruby, M.V.; Nicholson, A. Micromineralogy of mine wastes in relation to lead bioavailability, Butte, Montana. *Environ. Sci. Technol.* **1993**, *27*, 1415–1425. [[CrossRef](#)]
35. Alpers, C.N.; Rye, R.O.; Nordstrom, D.K.; White, L.D.; King, B. Chemical, crystallographic and stable isotopic properties of Alunite and Jarosite from acid—Hypersaline Australian lakes. *Chem. Geol.* **1992**, *96*, 203–226. [[CrossRef](#)]
36. Bigham, J.; Schwertmann, U.; Traina, S.; Winland, R.; Wolf, M. Schwertmannite and the chemical modeling of iron in acid sulfate waters. *Geochim. Cosmochim. Acta* **1996**, *60*, 2111–2121. [[CrossRef](#)]
37. Bothe, J.V.; Brown, P.W. Arsenic immobilization by calcium arsenate formation. *Environ. Sci. Technol.* **1999**, *33*, 3806–3811. [[CrossRef](#)]
38. Hongshao, Z.; Stanforth, R. Competitive adsorption of phosphate and arsenate on goethite. *Environ. Sci. Technol.* **2001**, *35*, 4753–4757. [[CrossRef](#)] [[PubMed](#)]
39. Jackson, B.P.; Miller, W. Effectiveness of phosphate and hydroxide for desorption of arsenic and selenium species from iron oxides. *Soil Sci. Soc. Am. J.* **2000**, *64*, 1616–1622. [[CrossRef](#)]
40. Manning, B.A.; Goldberg, S. Modeling competitive adsorption of arsenate with phosphate and molybdate on oxide minerals. *Soil Sci. Soc. Am. J.* **1996**, *60*, 121–131. [[CrossRef](#)]
41. Lindsay, W.L. *Chemical Equilibria in Soils*; John Wiley and Sons Ltd.: Hoboken, NJ, USA, 1979.
42. Zhang, J.; Stanforth, R. Slow adsorption reaction between arsenic species and goethite (α -FeOOH): Diffusion or heterogeneous surface reaction control. *Langmuir* **2005**, *21*, 2895–2901. [[CrossRef](#)] [[PubMed](#)]

43. Zhang, P.; Ryan, J.A. Formation of chloropyromorphite from galena (PbS) in the presence of hydroxyapatite. *Environ. Sci. Technol.* **1999**, *33*, 618–624. [[CrossRef](#)]
44. Burton, E.D.; Bush, R.T.; Sullivan, L.A.; Johnston, S.G.; Hocking, R.K. Mobility of arsenic and selected metals during re-flooding of iron-and organic-rich acid-sulfate soil. *Chem. Geol.* **2008**, *253*, 64–73. [[CrossRef](#)]
45. Garelick, H.; Jones, H.; Dybowska, A.; Valsami-Jones, E. Arsenic pollution sources. *Rev. Environ. Contam. Toxicol.* **2008**, *197*, 17–60. [[PubMed](#)]
46. Hansel, C.M.; Benner, S.G.; Fendorf, S. Competing Fe (II)-induced mineralization pathways of ferrihydrite. *Environ. Sci. Technol.* **2005**, *39*, 7147–7153. [[CrossRef](#)] [[PubMed](#)]
47. Burton, E.D.; Johnston, S.G.; Planer-Friedrich, B. Coupling of arsenic mobility to sulfur transformations during microbial sulfate reduction in the presence and absence of humic acid. *Chem. Geol.* **2013**, *343*, 12–24. [[CrossRef](#)]
48. Strawn, D.G.; Sparks, D.L. Effects of soil organic matter on the kinetics and mechanisms of Pb (II) sorption and desorption in soil. *Soil Sci. Soc. Am. J.* **2000**, *64*, 144–156. [[CrossRef](#)]
49. Kaštelan-Macan, M.; Petrovic, M. Competitive sorption of phosphate and marine humic substances on suspended particulate matter. *Water Sci. Technol.* **1995**, *32*, 349–355.
50. Zhou, S.; Song, Z.; Xu, M.; Chen, S. Effect of phosphate addition on mobility and phytoavailability of heavy metals in soils. In *Phosphate in Soils: Interaction with Micronutrients, Radionuclides and Heavy Metals*; CRC Press: Boca Raton, FL, USA, 2015; pp. 203–235.
51. Beak, D.G.; Basta, N.T.; Scheckel, K.G.; Traina, S.J. Bioaccessibility of lead sequestered to corundum and ferrihydrite in a simulated gastrointestinal system. *J. Environ. Qual.* **2006**, *35*, 2075–2083. [[CrossRef](#)] [[PubMed](#)]
52. Beak, D.G.; Basta, N.T.; Scheckel, K.G.; Traina, S.J. Linking solid phase speciation of Pb sequestered to birnessite to oral Pb bioaccessibility: Implications for soil remediation. *Environ. Sci. Technol.* **2007**, *42*, 779–785. [[CrossRef](#)]
53. Smith, E.; Weber, J.; Naidu, R.; McLaren, R.G.; Juhasz, A.L. Assessment of lead bioaccessibility in peri-urban contaminated soils. *J. Hazard. Mater.* **2011**, *186*, 300–305. [[CrossRef](#)] [[PubMed](#)]
54. Ying, S.C.; Kocar, B.D.; Fendorf, S. Oxidation and competitive retention of arsenic between iron-and manganese oxides. *Geochim. Cosmochim. Acta* **2012**, *96*, 294–303. [[CrossRef](#)]
55. Paktunc, D.; Majzlan, J.; Huang, A.; Thibault, Y.; Johnson, M.B.; White, M.A. Synthesis, characterization, and thermodynamics of arsenates forming in the Ca-Fe (III)-As (V)-NO₃ system: Implications for the stability of Ca-Fe arsenates. *Am. Mineral.* **2015**, *100*, 1803–1820. [[CrossRef](#)]
56. Smedley, P.; Kinniburgh, D. A review of the source, behaviour and distribution of arsenic in natural waters. *Appl. Geochem.* **2002**, *17*, 517–568. [[CrossRef](#)]
57. Stollenwerk, K. Geochemical processes controlling transport of arsenic in groundwater: A review of adsorption. In *Arsenic Ground Water*; Springer: Boston, MA, USA, 2003; pp. 67–100.
58. Pierce, M.L.; Moore, C.B. Adsorption of Arsenite and Arsenate on Amorphous Iron Hydroxide. *Water Res.* **1982**, *16*, 1247–1253. [[CrossRef](#)]
59. Wang, S.; Terdkiatburana, T.; Tadé, M. Adsorption of Cu (II), Pb (II) and humic acid on natural zeolite tuff in single and binary systems. *Sep. Purif. Technol.* **2008**, *62*, 64–70. [[CrossRef](#)]
60. Baron, D.; Palmer, C.D. Solid-solution aqueous-solution reactions between jarosite (KFe₃(SO₄)₂(OH)₆) and its chromate analog. *Geochim. Cosmochim. Acta* **2002**, *66*, 2841–2853. [[CrossRef](#)]
61. Kendall, M.R.; Madden, A.S.; Madden, M.E.E.; Hu, Q. Effects of arsenic incorporation on Jarosite dissolution rates and reaction products. *Geochim. Cosmochim. Acta* **2013**, *112*, 192–207. [[CrossRef](#)]

